Macromolecules **1992,** *25,* 1775–1779

Carbocationic Copolymerization in the Presence of Electron Pair Donors. 2. Copolymerization of Isobutylene and Isoprene or 2,4-Dimethyl-1,3-pentadiene with $TiCl_4$-Based Initiating Systems Yielding in Situ Electron Pair Donors

Gabor Kaszas,[†] Judit E. Puskas,[†] and J. P. Kennedy*

Institute of Polymer Research, University of Akron, Akron, Ohio 44325-3909

Received January 15, 1991; Revised Manuscript Received November 22, 1991

ABSTRACT: The copolymerization of the isobutylene (IB)–isoprene (IP) monomer pair by the cumyl acetate (CumOAc)/$TiCl_4$, cumyl propionate (CumOPr)/$TiCl_4$, and dicumyl methyl ether (DiCumOMe)/$TiCl_4$ initiating systems has been studied using CH_3Cl/n-C_6H_{14} (40 vol %/60 vol %) mixed solvent in the −30 to −80 °C range. Irreversible termination was absent in these systems, and the extent of chain transfer decreased with decreasing temperature. Cyclization of polyisoprene sequences is not detected even with 70 mol % IP in the charge. In contrast, with the CumOAc/BCl_3 initiating system irreversible termination was found at −40 °C and cyclization occurred beyond 20 mol % IP in the charge. IB–IP copolymer compositions determined by ^{1}H NMR spectroscopy are in good agreement with values calculated by the conventional reactivity ratios, $r_{IB} = 2.5$ and $r_{IP} = 0.4$. In line with the mechanism proposed for living IB polymerizations, it is suggested that CumOAc, CumOPr, or DiCumOMe in the presence of excess $TiCl_4$ give cumyl chloride (CumCl) or dicumyl chloride (DiCumCl), respectively, plus the corresponding in situ electron pair donors (ED) $TiCl_3OAc$, $TiCl_3OPr$, and $TiCl_3OMe$, and that the copolymerizations are induced by the Cum^+ or $^+DiCum^+$ carbocations arising from CumCl or DiCumCl plus excess $TiCl_4$. The propagating centers are in rapid equilibrium with dormant polymeric chlorides. The very similar apparent activation enthalpy differences of chain transfer and propagation calculated from parallel Arrhenius plots of the highest theoretically obtainable molecular weights—$\ln (1/\bar{M}_{n,lim})$ versus reciprocal temperatures—for *tert*-ester (CumOAc and CumOPr)/$TiCl_4$ and *tert*-ether (DiCumOMe)/$TiCl_4$ initiated IB–IP copolymerizations ($\Delta(\Delta H)$ = 5.1 and 4.6 kcal/mol, respectively) indicate that initiation and propagation occur by a common species, while the different apparent activation entropy differences ($\Delta(\Delta S)$ = 3.2 and 1.6 cal/K·mol) are most likely due to the different in situ EDs arising from the different initiators. Living copolymerization leading to soluble random copolymers has been obtained with the IB/2,4-dimethyl-1,3-pentadiene (DMPD) system. Internal strain and steric hindrance by the three methyl groups of the conjugated diene facilitate propagation and prevent chain transfer. In contrast to IB–IP copolymerizations, rate deceleration was not observed with IB–DMPD systems and IB–DMPD copolymers were found to be richer in DMPD than charged at incomplete conversions.

A. Introduction

The copolymerization of IB and IP induced by the CumOAc/BCl_3 system has recently been reinvestigated,[1] and the proposition in regard to the living nature of the CumOAc/BCl_3/IB–IP/CH_3Cl/−30 °C copolymerization[2] has been questioned. While the in situ electron pair donor (ED) BCl_2OAc, arising from the CumOAc/BCl_3 system,[3] leads to living IB homopolymerization under certain conditions,[4] it does not yield living IB–IP copolymerization. Therefore, it was of interest to explore the effect of different in situ EDs arising in *tert*-ester and *tert*-ether/$TiCl_4$ initiating systems[1] on IB–IP copolymerizations.

This paper concerns IB–IP and IB–DMPD copolymerizations induced by the CumOAc/$TiCl_4$, CumOPr/$TiCl_4$, and DiCumOMe/$TiCl_4$ initiating systems giving rise to the in situ EDs $TiCl_3OAc$, $TiCl_3OPr$, and $TiCl_3OMe$, respectively. The interpretation of the copolymerization data was greatly facilitated by the new mechanism proposed for living IB polymerizations.[3] While irreversible termination was absent, IB–IP copolymerization systems exhibited chain transfer even at −80 °C, although the extent of transfer was considerably smaller than that at −40 °C. In contrast, the IB–DMPD system yielded living random copolymerizations at −40 and −60 °C.

B. Experimental Section

B.1. Materials. The syntheses and purification of *2-phenyl-2-acetoxypropane* (cumyl acetate, CumOAc) and *2-phenyl-2-propionyloxypropane* (cumyl propionate, CumOPr) have been reported.[4,5] The purity of the products was checked by ^{1}H NMR spectroscopy. *1,4-Bis(2-methoxy-2-propyl)benzene* (p-dicumyl methyl ether, DiCumOMe) was synthesized as described[6] and purified by chromatography on neutral Al_2O_3 (Brockman activity III). Upon elution with n-pentane pure DiCumOMe was obtained. The purity was ascertained by DSC analysis (mp = 49 °C[7]). Sources and purification of *CH_3Cl, n-C_6H_{14}, IB,* and *$TiCl_4$* have been reported.[5] *IP* (Aldrich) was treated with 10% aqueous NaOH to remove the inhibitor, washed with distilled water until neutral, dried over anhydrous $CaCl_2$, and distilled from CaH_2 under N_2 on the day of the experiment. *DMPD* (Aldrich) was column chromatographed on neutral Al_2O_3 (Brockman activity I) in n-pentane solution to remove carbonyl-containing impurities, the eluent was dried over anhydrous $CaCl_2$, n-pentane was removed by rotavap, and the monomer was vacuum-distilled from CaH_2.

B.2. Procedures. Copolymerization and characterization procedures were identical to those used in IB homopolymerizations.[1–3] Detailed concentration, etc., data are given in the text and table or figure captions. Copolymer compositions were determined by ^{1}H NMR spectroscopy by comparing signal intensities of the aromatic initiator fragment (7.2 ppm, 5 H of cumyl, and 4 H of dicumyl) incorporated into the copolymer relative to those of the methine protons (5.12 ppm, 1 H) in the IP or DMPD units.

C. Results and Discussion

C.1. IB–IP Copolymerizations by the CumOAc/$TiCl_4$, CumOPr/$TiCl_4$, and DiCumOMe/$TiCl_4$ Initiating Systems. C.1.1. Experiments with 2.5 mol % IP in the Charge. Copolymerizations were carried out by the CumOAc/$TiCl_4$, CumOPr/$TiCl_4$, and DiCumOMe/$TiCl_4$ initiating systems in CH_3Cl/n-C_6H_{14} (40 vol

---

* Author to whom correspondence should be addressed.

[†] Present address: Polysar Rubber Corp., P.O. Box 3001, Sarnia, Ontario, Canada N7T 7M2.

0024-9297/92/2225-1775$03.00/0

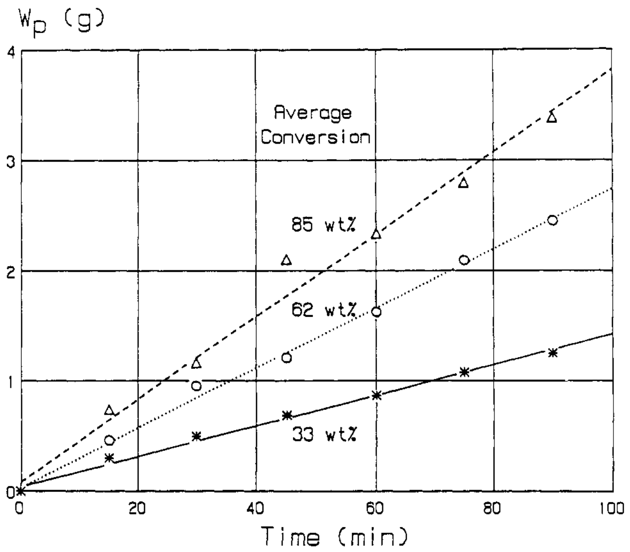

Figure 1. Weight of copolymer (W_p)-time plots of IB-IP copolymerizations initiated by the DiCumOMe/TiCl$_4$ system at -40 (*), -60 (○), and -80 °C (△). Conditions in Table I.

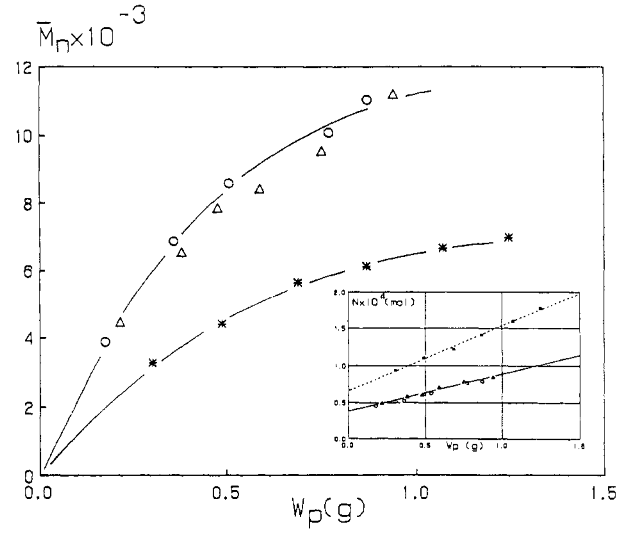

Figure 2. $\bar{M}_n$-W_p and N-W_p (inset) plots of IB-IP copolymerizations initiated by CumOAc/TiCl$_4$ (○), CumOPr/TiCl$_4$ (△), and DiCumOMe/TiCl$_4$ (*) at -40 °C. Conditions in Table I.

%/60 vol %) by the IMA technique[4] in the -30 to -80 °C range. The charges remained homogeneous throughout the experiments. Figure 1 shows the weight of copolymer W_p plotted against reaction time for the DiCumOMe/TiCl$_4$ initiating system at various temperatures. The W_p-time plots are linear, indicating the absence of irreversible chain termination. In contrast, termination was found to operate in CumOAc/BCl$_3$ initiated IB-IP copolymerizations.[1] The rate of copolymerizations decreased with increasing temperature, suggesting an ionic polymerization.

Figure 2 shows representative $\bar{M}_n$-W_p plots at -40 °C. The nonlinear character of the plots and the positive slopes of the number of polymer moles (N)-W_p plots (see inset in Figure 2) indicate chain transfer. The increase of N with W_p is less significant at lower temperatures, but positive slopes were obtained even at -80 °C.

Chain transfer limits the theoretically obtainable highest molecular weights ($\bar{M}_{n,\lim}$; see Table I). Since initiation is fast compared to propagation, $\bar{M}_n$ will increase with time at the early stages of the polymerization but eventually will reach a limit determined by the ratio of the propagation and transfer rates.

This theoretically obtainable highest molecular weight, $\bar{M}_{n,\lim}$, can be derived by searching for the maximum of eq 1 where $\bar{M}_n(t)$ is the molecular weight of a copolymer

$$\bar{M}_n(t) = W_p(t)/N(t) \tag{1}$$

at time t, $W_p(t)$ is the weight of copolymer formed at t, and $N(t)$ is the number of copolymer moles in the system at time t. $M_{n,\lim}$ is found by solving

$$\mathrm{d}\bar{M}_n(t)/\mathrm{d}t = 0 \tag{2}$$

Since the W_p-t and N-t plots are linear, the following simple equation can be used

$$W_p = Rt \quad \text{and} \quad N = N_0 + \mathrm{Tr} \times t \tag{3}$$

where R is the overall rate of copolymerization, N_0 is the intercept of the N-t plot, and Tr is a constant characteristic of chain transfer. From eqs 2 and 3 the molecular weight limit, reached at time $t = t_{\lim}$ can be derived

$$\bar{M}_{n,\lim} = \frac{W_p(t_{1,\lim})}{N(t_{1,\lim})} = \frac{\dfrac{\partial W_p(t)}{\partial t}}{\dfrac{\partial N(t)}{\partial t}} = \frac{R}{\mathrm{Tr}} \tag{4}$$

That is

$$1/\bar{M}_{n,\lim} = \mathrm{Tr}/R \tag{5}$$

where Tr/R is the slope of the N-W_p plot.

$\bar{M}_{n,\lim}$ values calculated by eq 5 are listed in Table I. $\bar{M}_{n,\lim}$ increases with decreasing temperatures, which indicates decreasing chain transfer (smaller Tr). $\bar{M}_w/\bar{M}_n$ values were around 2 at -40 °C and decreased with increasing molecular weight at -60 and -80 °C (from 2 to 1.7 and from 2 to 1.5, respectively). The molecular weight distributions in quasiliving IB homo- and copolymerizations, i.e., in systems where dormant chains are in dynamic equilibrium with active species, are expected to decrease with increasing molecular weights; this phenomenon will be discussed elsewhere.[11]

The ^{1}H NMR spectra of samples prepared at -80 °C show only a broad resonance in the olefinic region at 5.1 ppm due to -C=C*H*-, which indicates that the dominant IP enchainment is 1,4. Samples prepared at higher temperatures show additional very weak resonances around 4.8 and 4.6 ppm, which may be due to 3,4- and/or 1,2-IP enchainment or to olefinic structures such as ~CH$_2$C(CH$_3$)=CH$_2$ formed by chain transfer. However, these signals were too broad and weak for definitive assignments. Similar to CumOAC/BCl$_3$ initiated copolymerizations,[1] IR spectroscopy failed to detect carbonyl groups in the copolymers.

Table I
IB-IP Copolymerization by the CumOAc/TiCl$_4$, CumOPr/TiCl$_4$, and DiCumOMe/TiCl$_4$ Initiating Systems[a]

temp, °C	CumOAc conv, %	CumOAc $\bar{M}_{n,\lim}$	CumOPr conv, %	CumOPr $\bar{M}_{n,\lim}$	DiCumOMe conv, %	DiCumOMe $\bar{M}_{n,\lim}$
-30	36	11 500[b,c]				
-40	28	19 700[c]	24	19 800[d]	33	10 500
			51	18 200		
			77	21 400[e]		
-60			55	52 400	62	25 000
-80			80	190 000	85	90 400

[a] [CumOAc]$_0$ = 6.3 × 10^{-5} mol (2.5 × 10^{-3} mol/L); [CumOPr]$_0$ = 1.20 × 10^{-4} mol (4.8 × 10^{-3} mol/L); [DiCumOMe]$_0$ = 1.28 × 10^{-4} mol (5.12 × 10^{-3} mol/L); TiCl$_4$/[initiator] = 16; V_0 = 26 mL of CH$_3$Cl/n-C$_6$H$_{14}$ (60 vol %/40 vol %); IP in the monomer charge = 2.5 mol %, IMA technique, 6 × (1 mL of IB-IP/15 min). Conversions are averages of those measured in the individual IMA reactors. [b] [CumOAc]$_0$ = 1.26 × 10^{-4} mol. [c] IMA technique, 6 × (1 mL of IB-IP/60 min). [d] [CumOPr]$_0$ = 5.5 × 10^{-5} mol. [e] [CumOPr]$_0$ = 2.4 × 10^{-4} mol.

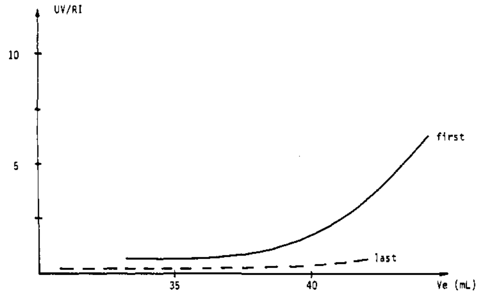

Figure 3. UV/RI ratios (GPC)–V_e plots of IB–IP copolymer samples prepared by the DiCumOMe/$TiCl_4$ system in the same IMA series at −80 °C. Conditions in Table I.

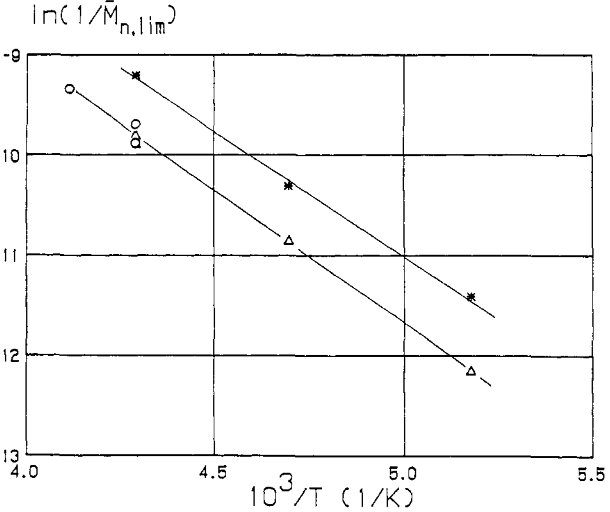

Figure 4. ln $(1/\bar{M}_{n,lim})$–$1/T$ plots of IB–IP copolymerizations initiated by CumOAc/$TiCl_4$ (○), CumOPr/$TiCl_4$ (△), and DiCumOMe/$TiCl_4$ (*) at −40 °C. Conditions in Table I.

The absence of irreversible termination and limited chain transfer of $TiCl_4$-coinitiated IB–IP copolymerizations at −80 °C is indicated by UV/RI–V_e plots, obtained from RI and UV (GPC) traces of the first and last copolymer sample of an IMA series (see Table I; −80 °C) shown in Figure 3. The intensities of the UV and RI traces at any elution volume are directly proportional to the number of chromophores (unsaturated IP units) and to the molecular weight of the sample, respectively, so the UV/RI ratio is proportional to the distribution of IP units as a function of the molecular weight. The UV/RI–V_e plot of the first sample shows that initially more IP units are in the short chains; this is in line with the conventional reactivity ratios, $r_{IB} = 2.5$ and $r_{IP} = 0.4$,[9,10] and with the observation that IB–IP copolymerizations are slower than IB homopolymerizations under identical conditions.[3,5] At longer polymerization times living propagation should yield a random IP distribution along the copolymer chains, i.e., horizontal UV/RI–V_e plots due to increasing molecular weights.[8] The almost horizontal UV/RI–V_e plot of the last copolymer sample shown in Figure 3 indicates limited chain transfer; in contrast, IB–IP copolymerizations initiated by CumOAc/BCl_3 yielded an increasingly heterogeneous distribution of IP units with increasing reaction time, due to extensive transfer.[1]

Figure 4 shows ln $(1/\bar{M}_{n,lim})$–$1/T$ plots constructed with the data in Table I. The data corresponding to the two different *tert*-esters (CumOAc or CumOPr)/$TiCl_4$ seem to define a distinctively different linear plot from those corresponding to the *tert*-ether (DiCumOMe)/$TiCl_4$. The two plots run parallel, indicating that the apparent activation enthalpy differences between propagation and transfer for these initiators are very similar ($\Delta(\Delta H) = 5.1$ and 4.6 kcal/mol, respectively). This suggests that propagation proceeds by analogous intermediates (poly(IB–IP)$^+TiCl_5^-$), regardless of the initiating complexes. The disparity in the intercept, that is, in the activation entropy differences ($\Delta(\Delta S) = 3.2$ and 1.6 cal/K·mol, respectively), probably reflects the structural difference between the in situ EDs, i.e., $TiCl_3OAc$ or $TiCl_3OPr$ and $TiCl_3OMe$, forming from the initiating complexes.[3]

Table II
Composition of IB–IP Copolymers Prepared by the CumOAc/$TiCl_4$ System[a]

IP in the charge, mol %	unsaturation in the copolym, mol % found[b]	unsaturation in the copolym, mol % calcd[c]	$\bar{M}_n$
96	22	90	multimodal
90	21	78	multimodal
80	21	61	multimodal
66	38	44	1170
46	24	25	1600

[a] $[CumOAc]_0 = 7.4 \times 10^{-4}$ mol (4.8×10^{-3} mol/L); $[TiCl_4]/[CumOAc] = 16$; $V_0 = 152$ mL; $CH_3Cl/n\text{-}C_6H_{14}$ (40 vol %/60 vol %); 2 × (12 mL of IB–IP/30 min); −40 °C. [b] By ^1H NMR. [c] From $r_{IB} = 2.5$ and $r_{IP} = 0.4$.[9,10]

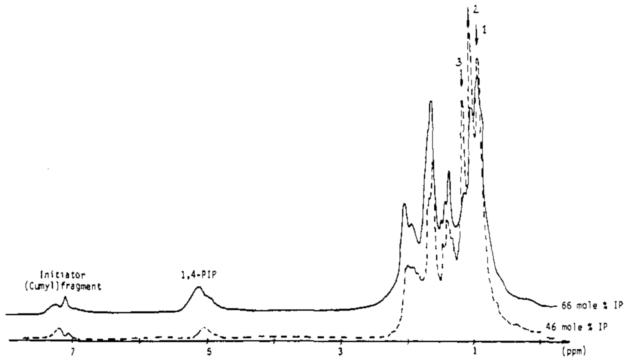

Figure 5. ^1H NMR spectra of IB–IB copolymers prepared by the $TiCl_4$ initiating system at −40 °C (last two samples in Table II). Conditions in Table II. (—) 66 mol % IP in the charge; conversion = 9%; $\bar{M}_n = 1170$, $\bar{M}_w/\bar{M}_n = 1.90$. (- - -) 46 mol % IP in the charge; conversion = 12%; $\bar{M}_n = 1600$, $\bar{M}_w/\bar{M}_n = 2.07$. (1) PBP (0.86 ppm); (B = IB; P = IP). (2) PBB or BBP (0.96 ppm). (3) BBB (1.11 ppm).

In summary, *tert*-ester/$TiCl_4$ and *tert*-ether/$TiCl_4$ initiated IB–IP copolymerizations are free of irreversible termination; however, chain transfer to monomer operates even at −80 °C, although its extent is greatly reduced at that temperature.

C.1.2. Experiments with 46–96 mol % IP in the Charge. Table II summarizes copolymer compositions obtained with high IP concentrations in the charge and the CumOAc/$TiCl_4$ system at −40 °C.

At higher than about 70 mol % IP in the charge, massive cyclization of the *trans*-1,4-polyisoprene sequences occurs.[12] In BCl_3-coinitiated IB–IP copolymerization, cyclization occurs already with 20 mol % IP in the charge.[2] Figure 5 shows the ^1H NMR spectra of the last two samples of Table II. The products are random copolymers and show no sign of cyclization. The resonances at 0.86, 0.96, and 1.11 ppm are characteristic of the PBP, PBB or BBP, and BBB triads (B = IB; P = IP), respectively.[13] With increasing IP content in the copolymer (from 24 to 38%) the relative intensities of the 1.11 and 0.96 ppm resonances decrease, leaving the PBP the dominant structure. Copolymer compositions calculated by the conventional $r_{IB} = 2.5$ and $r_{IP} = 0.4$ values[9,10] are in good agreement with the experimental data. Due to the complexity of the system (cyclization, penultimate effect, etc.), a single pair of r_1–r_2 values is insufficient to characterize IB–IP copolymerizations initiated by *tert*-ester and -ether/MtX_n

complexes,[1] and the calculated composition data provide only approximations.

In summary, the CumOAc/$TiCl_4$ initiating system in the mixed solvent CH_3Cl/*n*-hexane (40/60, v/v) at −40 °C produces soluble (gel-free) random IB–IP copolymers and does not induce cyclization of IP sequences in the 0–40 mol % copolymer composition range (i.e., up to 70 mol % IP in the charge).

C.2. IB–DMPD Copolymerization. C.2.1. Structural Considerations. Whereas the homopolymerization of IB by *tert*-ester or -ether/$TiCl_4$ initiating systems is living,[5,14] IB–IP copolymerization under identical conditions shows chain transfer. While the exact mechanism of this chain-transfer process is obscure, it certainly may involve H^+ loss via intramolecular cyclization.[2,15] We speculated that with DMPD the diene, chain transfer by cyclization would be prohibited because of steric compression:

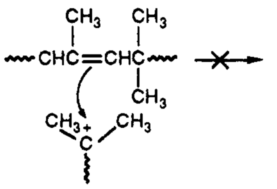

where the *tert*-carbenium ion may be due to the propagating PIB^+ or $DMPD^+$ and the approach may be intra- or intermolecular. In contrast, intra- or intermolecular cyclization readily proceeds in IB–IP copolymerization.[2,15]

DMPD incorporation in the chain will give a relatively stable *tert-tert*-allylic cation (versus the *tert-primary*-allylic character of an IP^+ chain end)

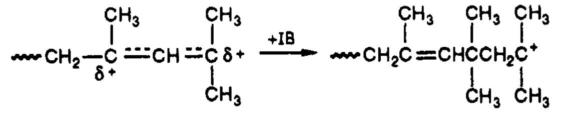

I

and after DMPD incorporation the ~DMPD–IB^+ propagating site will contain essentially the same internal strain (see formula above) as the conventional ~IB–IB^+ growing center (this strain is absent in the IP–IB^+ active center[1]). Also, these structural differences may result in faster cross-propagation (i.e., $PIB^+ + DMPD \rightarrow DMPD^+$ or $DMPD^+ + IB \rightarrow IB^+$) and therefore may lead to less H^+ elimination in IB–DMPD than in IB–IP copolymerization. Since H^+ loss is suppressed, the possibility of chain-transfer-less copolymerization arises.

C.2.2. Living Copolymerization of IB–DMPD. Keeping in mind the above structural considerations and in hope of attaining living conditions, IB–DMPD copolymerizations have been carried out with this monomer pair by the CumOAc/$TiCl_4$ and CumOPr/$TiCl_4$ initiating systems under various conditions. Figure 6 shows the results of experiments at −40 and −60 °C. The linear $\bar{M}_n$–W_p plot passing through the origin and corresponding horizontal N–W_p plot (inset) indicate living copolymerizations. The experiments at −60 °C yielded theoretical molecular weights with essentially 100% initiator efficiencies (I_{eff}) characteristic of a living copolymerization. The experiments at −40 °C gave lower than theoretical $\bar{M}_n$s (higher than theoretical Ns) most likely due to some adventitious initiation by protic impurities. Similar observations have been described for IB homopolymerizations at −40 °C.[5] The molecular weight distributions are relatively narrow and show a narrowing trend with increasing $\bar{M}_n$; for example, the copolymer with $\bar{M}_n$ = 66 300 shows $\bar{M}_w/\bar{M}_n$ = 1.18.

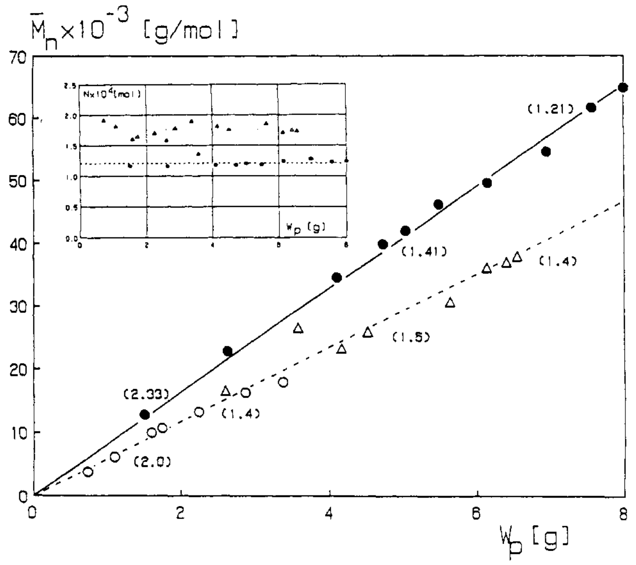

Figure 6. Copolymerization of IB with DMPD by the CumOAc/$TiCl_4$ system at −40 °C (○,△) and at −60 °C (●). Numbers in parentheses represent $\bar{M}_w/\bar{M}_n$ values. (○) Conditions are given in Table III. (△) $[CumOAc]_0 = 1.03 \times 10^{-4}$ mol (3.7×10^{-3} mol/L); $TiCl_4$/CumOAc = 8; $[IB]_0$ = 3.4 mol/L (10 mL); $[DMPD]_0 = 8 \times 10^{-2}$ mol/L (2.5 mol % in the charge); V_0 = 35 mL; polymerization times = 2, 3, 4, 5, 6, 7, 8, and 11.5 h. (●) $[CumOAc]_0 = 1.03 \times 10^{-4}$ mol (3.7×10^{-3} mol/L); $TiCl_4$/CumOAc = 8; $[IB]_0$ = 3.3 mol/L (12.5 mL); $[DMPD]_0 = 1 \times 10^{-1}$ mol/L (3 mol % in the charge); V_0 = 38 mL; polymerization times = 20, 40, 60, 80, 100, 120, 140, 160, 180, 200, and 220 min.

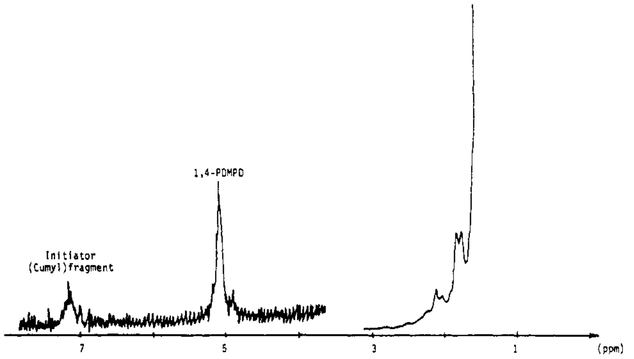

Figure 7. ^1H NMR spectrum of a IB–DMPD copolymer (first sample in Table III). Conditions in Table III.

The structure of the copolymers has been investigated by ^1H NMR spectroscopy. The spectrum of a representative sample is shown in Figure 7. Significantly, the spectrum exhibits only one resonance in the olefinic region at 5.1 ppm which is attributed to the ~$CH_2C(CH_3)$=$CHC(CH_3)_2$ unit.

Copolymer compositions have also been determined by ^1H NMR spectroscopy. As shown by the data in Table III, IB–DMPD copolymers obtained at less than 100% conversions contain more DMPD than the charge (for example, 3 mol % DMPD in the charge gave 9.1 mol % DMPD in the first copolymer sample at 16 wt % monomer conversion) and the DMPD is depleted before the IB is consumed.

The IB–DMPD copolymerization is faster than the IB–IP copolymerization. IB–IP and IB–DMPD mixtures containing 3 mol % diene were copolymerized by the CumOPr/$TiCl_4$ system ($[CumOPr]_0 = 1.25 \times 10^{-4}$ mol (4.8×10^{-3} mol/L), $TiCl_4$/CumOPr = 16, V_0 = 25 mL, IMA technique, 5 × (1 mL/15 min) at −60 °C. The IB–IP copolymerization gave an average of 55 wt % conversion while the IB–DMPD copolymerization yielded close to 100 wt % conversions in each reactor. The molecular

Table III
Composition Data of IB–DMPD Copolymers Obtained by the CumOAc/TiCl$_4$ Initiating System[a]

polymn time, h	W_p, g	conv(IB + DMPD), %	DMPD in polym,[b] mol %	DMPD conv,[c] %
0.5	0.727	16	9.1	46
1.0	1.085	23	8.8	64
1.5	1.586	34	6.3	69
2.0	1.738	37	5.9	70
2.5	2.238	48	5.1	79
3.0	2.878	61	5.0	99
3.5	3.388	73	3.4	82

[a] $[\mathrm{CumOAc}]_0 = 1.03 \times 10^{-4}$ mol (3.2×10^{-3} mol/L); TiCl$_4$/CumOAc = 8; $[\mathrm{IB}]_0 = 7.97 \times 10^{-2}$ mol (2.5 mol/L); $[\mathrm{DMPD}]_0 = 2.5 \times 10^{-3}$ mol (7.8×10^{-2} mol/L); 3 mol % in the charge; V_0 = 32 mL of CH_3Cl/n-C_6H_{14} (40 vol %/60 vol %); −40 °C. [b] By ^{1}H NMR. [c] Calculated from conversion and copolymer composition data.

Scheme I
Living Copolymerization of IB and DMPD

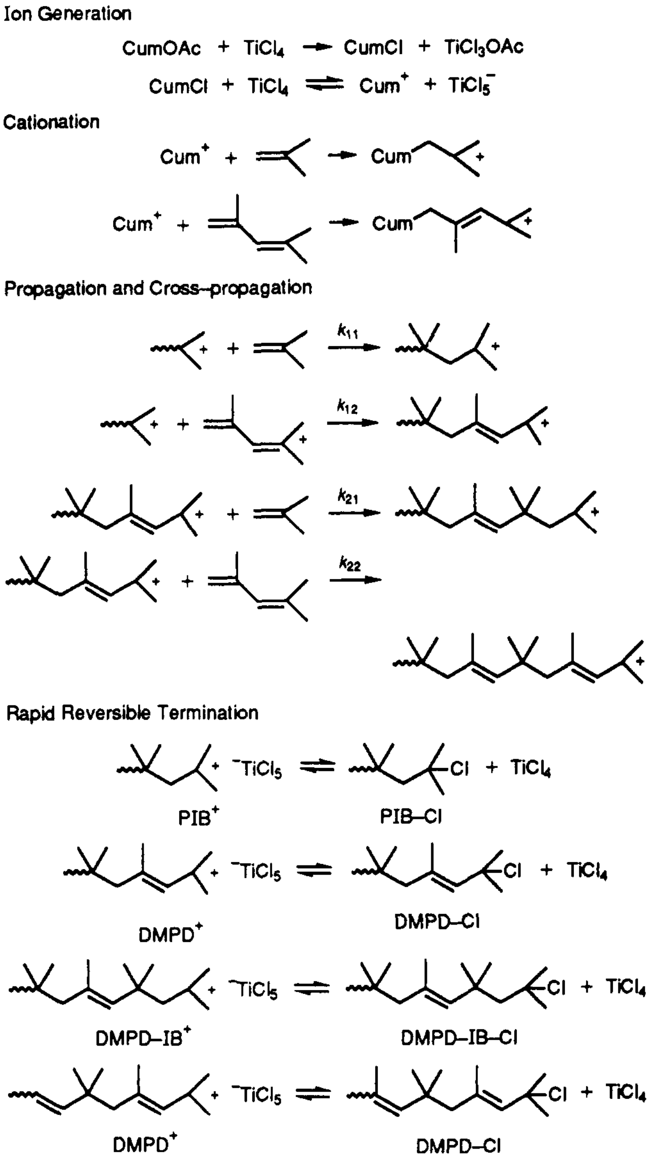

weight distributions became narrower in both cases with increasing molecular weight (i.e., from 2.07 to 1.79 with IB–IP and from 1.54 to 1.23 with IB–DMPD). The higher overall copolymerization rate of IB–DMPD is due to the above-discussed structural differences. The narrower MWD of IB–DMPD is probably due to the lower reactivity difference of this monomer pair.

A simplified mechanism of living copolymerization of IB–DMPD is outlined in Scheme I.

Ion generation, i.e., the formation of the initiating Cum$^+$ together with the formation of the in situ ED TiCl$_3$OAc, from *tert*-esters has been discussed in detail.[3,17] Cationation, propagation, and cross-propagation are visualized to proceed along conventional routes. The role of in situ EDs in mediating living carbocationic polymerizations has been extensively discussed.[3,17]

Provided the lifetimes of the active centers in the above three termination equilibria are sufficiently long relative to propagation, permanent termination will be absent. These equilibria are termed quasiliving equilibria and the associated termination steps quasiliving termination. The concept of quasiliving polymerization in general, and quasiliving termination in particular, has been discussed in detail.[16] In the second and fourth equilibria, DMPD$^+$ TiCl$_5^-$ → DMPD–Cl + TiCl$_4$, the retroreactions are expected to be particularly rapid because of the high reactivity of the terminal *tert*-allylic chloride and stability of the *tert*-*tert*-allylic cation DMPD$^+$ (for simplicity's sake only the terminal *tert*-allylic cation is shown). Similarly, in the first and third equilibria the internal strain stored in PIB–Cl and DMPD–IB–Cl promotes efficient reionization of the chloride by TiCl$_4$. The absence of permanent termination is one of the requirements of living polymerization.

The absence of chain transfer is most likely due to the formation during ion generation of the in situ ED, TiCl$_3$OAc; mediation of living carbocationic polymerization by in situ EDs has been discussed in detail.[3]

Acknowledgment. Useful suggestions by Dr. T. Pernecker are greatly appreciated. This material is based upon work supported by the National Science Foundation under Grant 89-20826.

References and Notes

(1) Part 1: Kaszas, G.; Puskas, J. E.; Kennedy, J. P. *Macromolecules*, previous paper in this issue.
(2) Faust, R.; Fehervari, A.; Kennedy, J. P. *Br. Polym. J.* **1987**, *19*, 379.
(3) Kaszas, G.; Puskas, J. E.; Chen, C. C.; Kennedy, J. P. *Macromolecules* **1990**, *23* (17), 3909.
(4) Faust, R.; Kennedy, J. P. *J. Polym. Sci., Polym. Chem. Ed.* **1987**, *25*, 1847.
(5) Kaszas, G.; Puskas, J. E.; Kennedy, J. P. *Makromol. Chem., Macromol. Symp.* **1988**, *13/14*, 473.
(6) Mishra, K. K.; Kennedy, J. P. *Polym. Bull.* **1987**, *17*, 7.
(7) Kaszas, G.; Puskas, J. E.; Kennedy, J. P. *J. Appl. Polym. Sci.* **1990**, *39*, 119.
(8) Stockmayer, W. H. *J. Chem. Phys.* **1945**, *13* (6), 199.
(9) Kennedy, J. P.; Canter, N. H. *Ann. N.Y. Acad. Sci.* **1969**, *155*, 419.
(10) Tudos, F.; Kelen, T.; Foldes-Berezsnich, T.; Turcsanyi, B. *J. Macromol. Sci., Chem.* **1976**, *A10* (8), 1513.
(11) Puskas, J. E.; Kaszas, G.; Litt, M. *Macromolecules* **1991**, *24*, 5278.
(12) Puskas, J. E.; Kaszas, G.; Kennedy, J. P. *Polym. Mater. Sci. Eng.* **1987**, *57*, 77.
(13) Corno, C.; Proni, A.; Priola, A.; Cesca, S. *Macromolecules* **1980**, *13*, 1092.
(14) Kaszas, G.; Puskas, J. E.; Kennedy, J. P. *Polym. Bull.* **1987**, *18*, 123.
(15) Kuntz, I.; Powers, K. W.; Hsu, C. S.; Rose, K. D. *Makromol. Chem., Macromol Symp.* **1988**, *13/14*, 337.
(16) Kennedy, J. P.; Kelen, T.; Tudos, F. *J. Macromol. Sci., Chem.* **1982–83**, *A18* (9), 1189.
(17) Kaszas, G.; Puskas, J. E.; Kennedy, J. P.; Chen, C. C. *Polym. Bull.* **1988**, *20*, 413.

Registry No. IB, 115-11-7; IP, 78-79-5; CumOAc, 3425-72-7; CumOPr, 114288-68-5; DiCumOMe, 37832-34-1; IB–IP (copolymer), 9010-85-9; DMPD, 1000-86-8; IB–DMPD (copolymer), 138983-67-2; TiCl$_4$, 7550-45-0.